Cell Prolif. 1999, **32**, 303–319

Degradation of apoptotic cells and fragments in HL-60 suspension cultures after induction of apoptosis by camptothecin and ethanol

H. Baisch, H. Bollmann and S. Bornkessel

Institute of Biophysics and Radiobiology, University of Hamburg, Germany

(*Received* 21 *October* 1998; *second revision accepted* 21 *June* 1999)

Abstract. Early indicators of apoptosis in mammalian cells are membrane potential breakdown (loss) in mitochondria (MPLM), chromatin condensation, DNA degradation, and phosphatidylserine exposure (PSE) on the outside plasma membrane. One aim of the present study was to determine the kinetics of these characteristics. These changes were measured by flow cytometry using the following methods: membrane potential of mitochondria was analysed using Mito Tracker Green and Red, PSE was analysed using annexin-V-FITC staining simultaneously with propidium iodide (PI) to detect membrane permeability; chromatin condensation was measured using the acid denaturation Acridine Orange (AO) method; DNA degradation was studied by the sub G_1 method and the terminal transferase dUTP nick end-labelling (TUNEL) assay (labelling of strand breaks). HL-60 cells were induced to apoptosis by 3% ethanol and 1.5 μM camptothecin (CAM) and the kinetics of the apoptotic cells were measured. The same kinetics were found for chromatin condensation and DNA degradation indicating that these changes appeared at approximately the same time after induction. The MPLM and PSE kinetics showed a considerably later increase indicating that MPLM occurred downstream of DNA degradation and that plasma membrane changes occurred downstream of MPLM.

The main aim of the study was to follow the fate of apoptotic cells after the appearance of the initial characteristics. The lifetime of apoptotic cells was studied by chase experiments. The inducing drug was removed after 4 h treatment and the disappearance of apoptoses recorded. An exponential decay was measured with a half life ($T_{½}$) of 17.8 h. As a corollary from these experiments, camptothecin was found to induce apoptosis also in G_1 and G_2 phase cells, however, it took much longer to occur than in S phase cells.

Using labelling of the plasma membrane with a fluorescent cell membrane linker, it was possible to show that the majority of apoptotic bodies as well as condensed apoptotic cells contain DNA and membrane. The degradation of these apoptotic bodies follows similar kinetics as those of the condensed apoptotic cells. The membrane remained considerably stable, there was no further loss in the next

Correspondence: H. Baisch, Institute of Biophysics and Radiobiology, University of Hamburg, Martinistrasse 52, 20246 Hamburg, Germany. E-mail: baisch@uke.uni-hamburg.de

7 days, after the first day when the apoptotic characteristics develop. It is concluded that the apoptosis programme is completed within a day and no further steps follow.

INTRODUCTION

Apoptosis is a common mode of programmed cell death occurring in tissue development and differentiation as well as during tumour growth (for review see Wyllie 1992, Majno & Joris 1995). A special interest in apoptosis in oncology originates from the observation that several anti-tumour drugs induce apoptosis (Darzynkiewicz 1995, Fisher 1994, Kerr, Winterford & Harmon 1994). There is evidence that in leukaemic cells the efficiency of a drug treatment can be monitored by measuring the number of apoptoses (Frankfurt *et al.* 1993, Li *et al.* 1994).

During the apoptosis process, a cascade of special biochemical events is triggered leading to specific morphological changes in the cell nucleus and in the cytoplasm (Mignotte & Vayssiere 1998, Thompson 1998). However, the sequential occurrence of these processes and in particular, the exact pathway of events is less clear. A number of apoptosis assays have been developed that are based on the different molecular, physiological and morphological changes the cells undergo on their way from a healthy state to apoptotic death (Darzynkiewicz *et al.* 1992, Frey 1997). In the cell membrane, phosphatidylserine, which is predominantly located on the inner leaflet of the plasma membrane in normal cells, is translocated to the outer side when cells become apoptotic. This can be measured by annexin-V attached to fluorescein isothiocyanate (FITC) fluorochrome (Boersma *et al.* 1996, Van Engeland *et al.* 1998). Moreover, the membrane becomes permeable for dyes like HO 33258 and propidium iodide (PI) (Zamai *et al.* 1996). The mitochondrial membrane potential is reduced in apoptotic cells, which can be measured by staining the cells with the membrane potential sensitive dye 'Mito Tracker' (Poot, Gibson & Singer 1997). In the cell nucleus, chromatin condensation is one of the prominent features in apoptotic cells (Hotz, Traganos & Darzynkiewicz 1992). This condensation is very likely related to the degradation of the DNA, caused by activation of endogenous nucleases. DNA degradation can be measured by various methods, such as electrophoresis ladder, terminal transferase nick end-labelling (TUNEL), and the sub-G_1 peak in flow cytometry (Hotz *et al.* 1994). Membrane blebbing and the formation of membrane-wrapped vesicles, the apoptotic bodies, were among the first features associated with apoptosis (Kerr *et al.* 1972). The sequence of appearance of these morphological and biochemical events may help to reveal the pathway of signals leading to apoptosis.

Most of the above features appear early, within a few hours, after induction of cells to apoptosis. Whether the programme of cell death extends beyond DNA degradation, chromatin condensation and the formation of apoptotic bodies has not been studied to date. Cells becoming apoptotic in a solid tissue disappear by phagocytosis. The condensed nuclei and apoptotic bodies are engulfed by macrophages or their neighbouring cells (Bursch *et al.* 1990). The lifetime of apoptotic features is very short, which represents a problem when the rate of apoptosis is estimated. White blood and leukaemic cells becoming apoptotic may have a longer lifetime, however, this cannot readily be measured *in vivo*. *In vitro*, in a cell culture, the lifetime of apoptotic bodies and condensed cell nuclei can be studied without phagocytosis in chase experiments.

The aims of the present study were (i) to investigate whether the sequence of appearance of the various apoptotic characteristics is different when completely different inducers of apoptosis such as ethanol and CAM are used and (ii) to follow the fate of apoptotic cells

(bodies) until their eventual decomposition. Apoptosis induced by ethanol and CAM was studied in HL-60 cells. The putative primary effect of ethanol is a change in membrane permeability, whereas CAM is an inhibitor of topoisomerase I in the cell nucleus. Methods allowing the measurement of the sequence of appearance of membrane changes, chromatin condensation, and DNA degradation were used. In extended time experiments, the decomposition of condensed cells and apoptotic bodies was examined. The half life of these apoptotic particles was about 18 h, which is much longer than the processes occurring during induction of apoptosis. To reveal if the apoptotic cells and bodies loose or keep their membrane, a membrane marker (PKH) was introduced into the cells before they were induced to apoptosis. The results indicate that condensed cells and apoptotic bodies are remarkably stable and retain their membrane relatively intact over a long period of time. One implication of these observations is that after chromatin condensation/DNA degradation and formation of apoptotic bodies and dense cell nuclei, no, or only slow, steps follow in the apoptotic programme until decomposition.

MATERIALS AND METHODS

Cells

HL-60 cells were obtained from the American Tissue Type Association (Bethesda, MD, USA) and maintained in RPMI 1640 medium (GIBCO BRL, Eggenstein, Germany) supplemented with 10% fetal calf serum, 200 U/ml penicillin, 100 μg/ml streptomycin, and 2 mM *l*-glutamine.

Apoptosis induction

The cells were induced to apoptosis by 1.5 μM CAM (Sigma, St Louis, MO, USA), or 3% ethanol. Stock solutions of CAM were prepared at a drug concentration of 2 mM in dimethylsulphoxide, and 3.75 μl were added to 5 ml cell suspension to give a concentration of 1.5 μM. In the chase experiments, the cells were centrifuged after 4 h of treatment and re-suspended with fresh medium.

Staining methods for apoptosis

Cells were stained to measure four different characteristics of apoptotic cells: (1) membrane changes, (2) chromatin sensitivity, (3) DNA breaks, and (4) loss of membrane potential in mitochondria.

1 To assess plasma membrane changes, the live cells were stained with annexin-V-FITC and PI according to the manufacturer's instructions (Clontech, Palo Alto, CA, USA). Briefly, the cells were washed in phosphate-buffered saline (PBS), incubated in binding buffer with annexin-V-FITC and PI for 15 min in the dark and measured on a FACScan (Becton Dickinson, San Jose, CA, USA).

2 To assess the chromatin condensation, the sensitivity of DNA *in situ* to denaturation was tested according to the method of Darzynkiewicz (1990). The cells were fixed with 80% ethanol at −20°C and stored. For staining they were centrifuged, resuspended in 0.1% RNase, incubated at 37°C for 15 min, centrifuged, treated with 0.1 M HCl for 20 min, and stained with 0.4 μg/ml Acridine Orange (AO; Polyscience Europe, Eppelheim, Germany) in citric acid/phosphate at pH 2.6. The cells were analysed in a FACScan within 10 min of staining.

3 Occurence of DNA-breaks were measured using the sub-G_1 peak method and the DNA strand break TUNEL assay (Hotz *et al.* 1994). For the sub-G_1 method, cells were fixed in

70% ethanol at −20°C, resuspended in 30 mM phosphate buffer to extract low molecular weight DNA, and stained with 50 μg/ml PI together with 0.05 mg/ml RNase A (SERVA, Heidelberg, Germany). The cells were fixed in 1% formaldehyde and post-fixed in 70% ethanol at −20°C for the TUNEL assay, washed in PBS and resuspended in 50 μl of a buffer solution containing 0.2 M potassium cacodylate, 2.5 mM Tris–HCl (pH 6.6), 2.5 mM $CoCl_2$, 0.25 mg/ml bovine serum albumin, 5 units of terminal deoxynucleotidyl transferase, and 10 μM of biotinylated dUTP (Boehringer Mannheim, Mannheim, Germany). After incubation at 37°C for 30 min, the cells were rinsed in PBS, resuspended in a saline–sodium citrate buffer with 2.5 μg/ml fluorescein-avidin (Boehringer Mannheim), 0.1% Triton X-100 (Sigma, St Louis, MO, USA), and 10% non-fat dried milk (Merck, Darmstadt, Germany), incubated for 30 min at room temperature in the dark, rinsed and resuspended in 5 μg/ml PI and 1 mg/ml RNase A.

4 Mitochondria membrane potential assay (Poot *et al.* 1997). Briefly, Mito Tracker Green FM and Red CMX Ros (Molecular Probes, Eugene, OR, USA) were added to viable cells in medium to a final concentration of 100 nM each and incubated for 20 min at 37°C, then chilled in ice and measured in the FACScan. Mito Tracker green fluorescence intensity is proportional to the total mass of mitochondria while the red fluorescence intensity of Red CMX Ros is related to the membrane potential of the mitochondria.

PKH labelling of cell membranes

HL-60 cells were labelled with PKH2-GL fluorescent cell membrane linker (Sigma) according to Horan *et al.* (1990). Briefly, 2×10^7 cells were washed in medium without serum, stained with PKH 2-GL, centrifuged through serum to remove unbound dye solution, and resuspended in medium with 10% serum. One culture without PKH2-GL served as a negative control of the PKH labelling. For apoptosis induction, ethanol was added to a PKH-labelled culture as described above, and another PKH-labelled culture served as the untreated control. Two parallel FACScan measurements were performed with FSC linear and logarithmic, respectively. The log-FSC measurement included small particles like cell fragments and apoptotic bodies.

Flow cytometry

All flow cytometry measurements were performed with a FACScan Flow Cytometer (Becton Dickinson). Five thousand cells per sample were collected using FACScan software, data analysis was in part done with DAS software kindly provided by W. Beisker, GSF, Oberschleißheim, Germany.

RESULTS

Induction of apoptosis

The appearance of the following apoptotic characteristics: (1) exposure of phosphatidylserine (PS) on the outside of the cell membrane, measured by annexin-V-FITC; (2) mitochondiral membrane break down, measured by Mito Tracker; (3) chromatin condensation measured by AO staining; and (4) DNA degradation measured by the sub-G_1 method and TUNEL were measured through various time spans after the induction of apoptosis (see *Material and methods*). The percentage of apoptotic cells could be quantitatively determined with all methods. In Figure 1 the per cent apoptosis data are plotted vs. time. While DNA degradation and changes in chromatin structure appear at the same time after induction, the

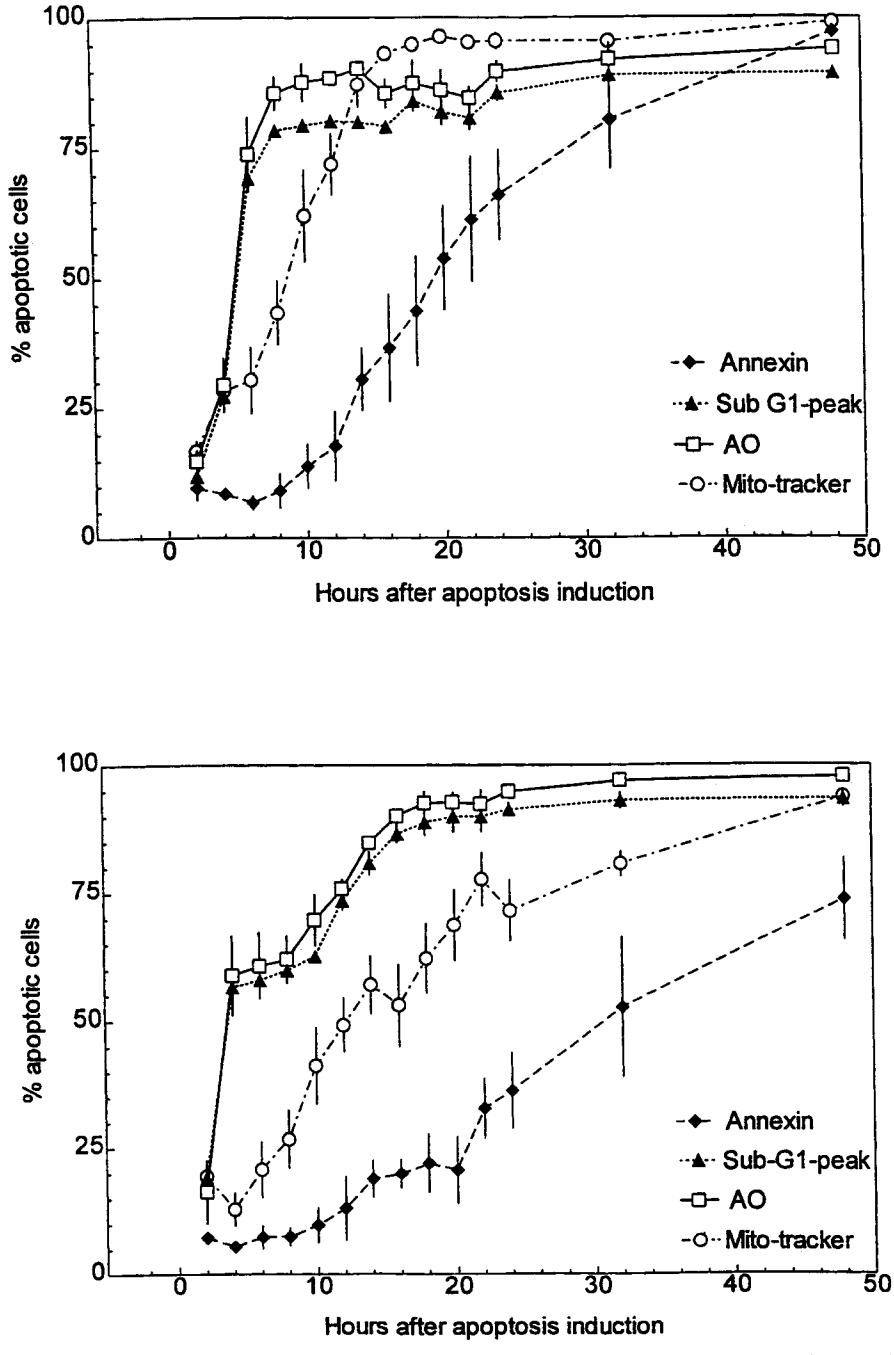

Figure 1. Kinetics of induction of apoptosis as measured by annexin-V-PI (membrane changes), Acridine Orange (chromatin condensation), sub-G_1 peak (DNA breaks), and Mito Tracker (reduction of mitochondria membrane potential). Top panel: induction of cells to apoptosis by ethanol, bottom panel: induction by camptothecin.

damage to the mitochondria membrane potential follows approximately 4 h later, and the translocation of PS to the outer surface as well as a slight increase of plasma membrane permeability appear several hours later and occur much more slowly.

Degradation kinetics of apoptotic cells

Under the microscope, some apoptotic cells showed typical nuclear fragmentation, however, many other cells appeared with a densely stained nucleus and these cells remained in the culture for more than 3 days. To assess the kinetics of apoptotic cell degradation, chase experiments were performed where the induction chemical was removed after 4 h treatment and the cells were resuspended in the medium in which they had been cultured. When the induction chemical is present permanently, the induction of apoptosis may be delayed in some cells and those late-onset apoptotic cells will obscure the degradation kinetics. In the chase experiment, it was necessary to determine whether the process of apoptosis induction is stopped after withdrawal of the induction chemical. Figure 2 shows dot plots of cells treated with CAM for 4 h and measured 6 and 14 h after the termination of treatment, respectively. After 6 h, only S phase cells are apoptotic (Figure 2a: large green fluorescence and DNA content (red fluorescence) between the G1 and G2 positions), however, after 14 h nearly all the cells have become apoptotic (Figure 2b: majority of cells have high green fluorescence). This indicates that cells treated with CAM in the G_1 phase become apoptotic about 10 h later. Up to 12 h after the end of treatment, only S phase cells were apoptotic, at later times the percentage of apoptotic cells increased slowly, including cells treated in the G1 phase. Measurements using the TUNEL method were performed at fewer time intervals. The percentage of apoptotic cells was always close to that obtained with AO or the sub G_1 peak methods. As the CAM treated cells continued to become apoptotic during an extended time span after removal of CAM, it was not feasible to study their degradation.

The cells induced to apoptosis by ethanol showed a different behaviour. In Figure 3 (upper panel) it can be seen that ethanol-treated cells start to grow again after the removal of ethanol and with the same doubling time as control cells indicating that all cells which were viable at the end of the treatment remained viable. The percentage of apoptoses decreased immediately after the termination of ethanol treatment (Figure 3, lower panel), while the percentage of live cells increases as a result of proliferation (the upper curve in the upper panel includes both apoptotic and live cells). The kinetics of apoptotic cell degradation was calculated from the total cell number and the percentage of apoptoses and is plotted in the upper panel (lower curve). It was an exponential decay with a half life ($T_{½}$) of 17.8 h in this experiment. Two repeated experiments resulted in $T_{½}$ of 18.3 and 16 h. The mean $T_{½}$ value for degradation of apoptotic cells from the 3 experiments was 17.6 ± 0.9 h.

Membrane status of apoptotic cells and fragments

To assess whether the apoptotic cells and fragments retain their membranes, HL-60 cells were labelled with fluorescent linker (PKH2-GL). Figure 4 (upper left panel) shows cells directly after labelling to have an intense green fluorescence and low PI-fluorescence. After 7 days (upper right panel), the green fluorescence has decreased by about a factor of 50 as a result of cell division and hence dilution of PKH-label. The dead apoptotic cells at high PI fluorescence show about half the green fluorescence of the live cells owing to shrinkage and partial loss of membrane. After 1 day of ethanol treatment (Figure 4, lower left panel), the majority of cells maintain membrane integrity with respect to PI uptake. However, more than 50% of the cells show decreased PKH-fluorescence, indicating cell shrinkage or loss of

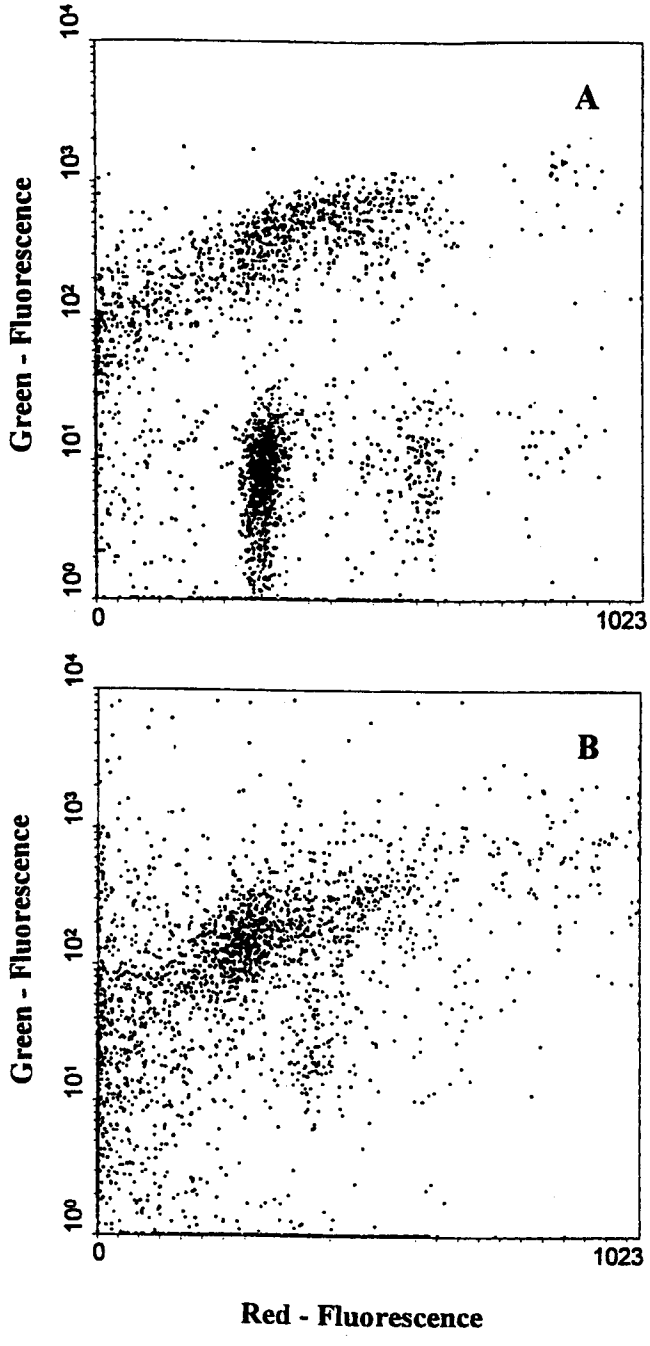

Figure 2. Dot plots of HL-60 cells treated with 1.5 μm camptothecin for 4 h, then incubated with fresh medium. Cells were double stained using the terminal transferase (TUNEL) method for apoptotic cells (green) and PI for DNA content (red fluorescence). (a) 6 h, (b) 14 h after termination of camptothecin treatment. In control cells the green fluorescence of S phase cells appears at the level of G_1 and G_2 cells.

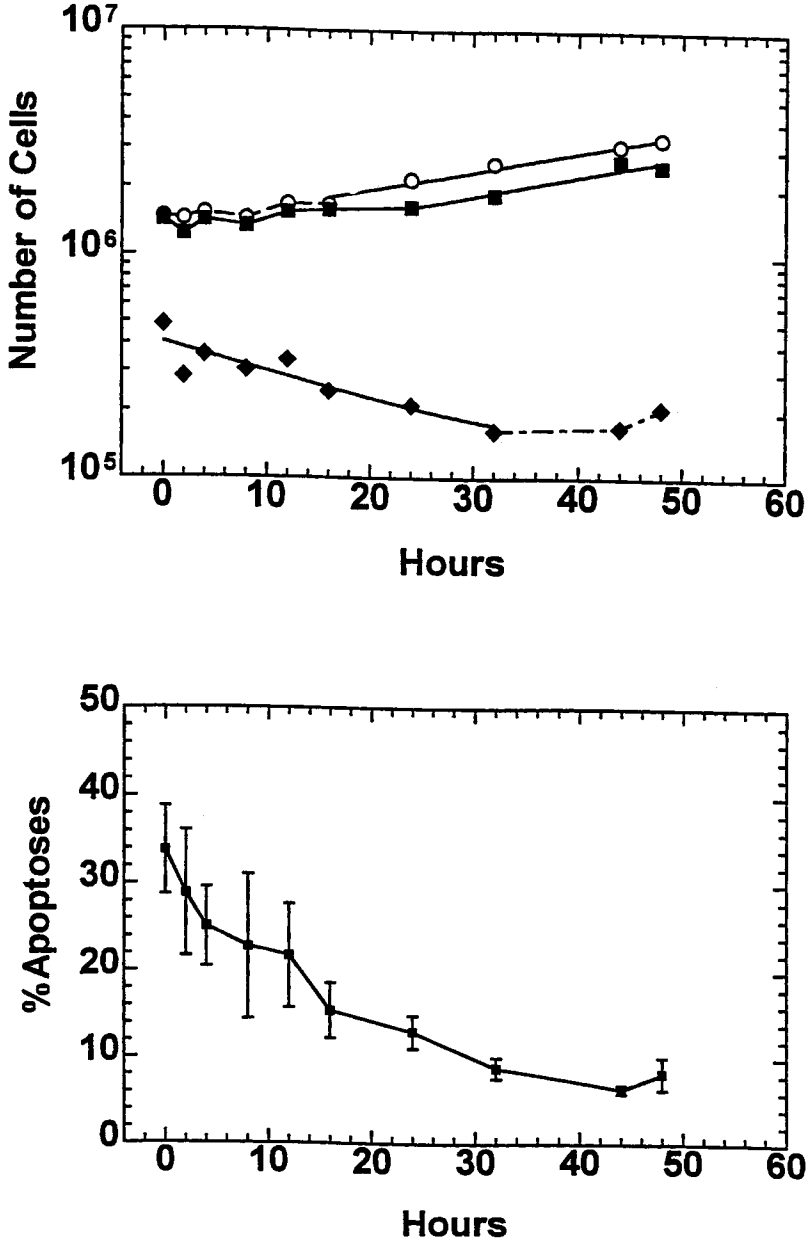

Figure 3. Growth of HL-60 cells treated for 4 h with 3% ethanol. Immediately after treatment 34% ± SD of the cells are apoptotic as measured using Acridine Orange, sub-G_1 and morphology methods, which showed the same kinetics. The lower panel shows the means and standard deviations calculated from the results of the 3 methods. With time the percentage of apoptotic cells decreases, however, part of this decrease is due to the growth of the non-apoptotic surviving cells. In the upper panel the growth curve of ethanol-treated cells (■) is shown to be parallel to the control growth curve (○), only at a lower level. The doubling times T_d are 35.1 h for the control cells and 34.0 h for the ethanol-treated cells. The number of apoptotic cells (◆), calculated from the total number and the percentage of apoptotic cells shown in the lower panel, decreases exponentially up to 32 h, with a half life ($T_{½}$) of 17.8 h.

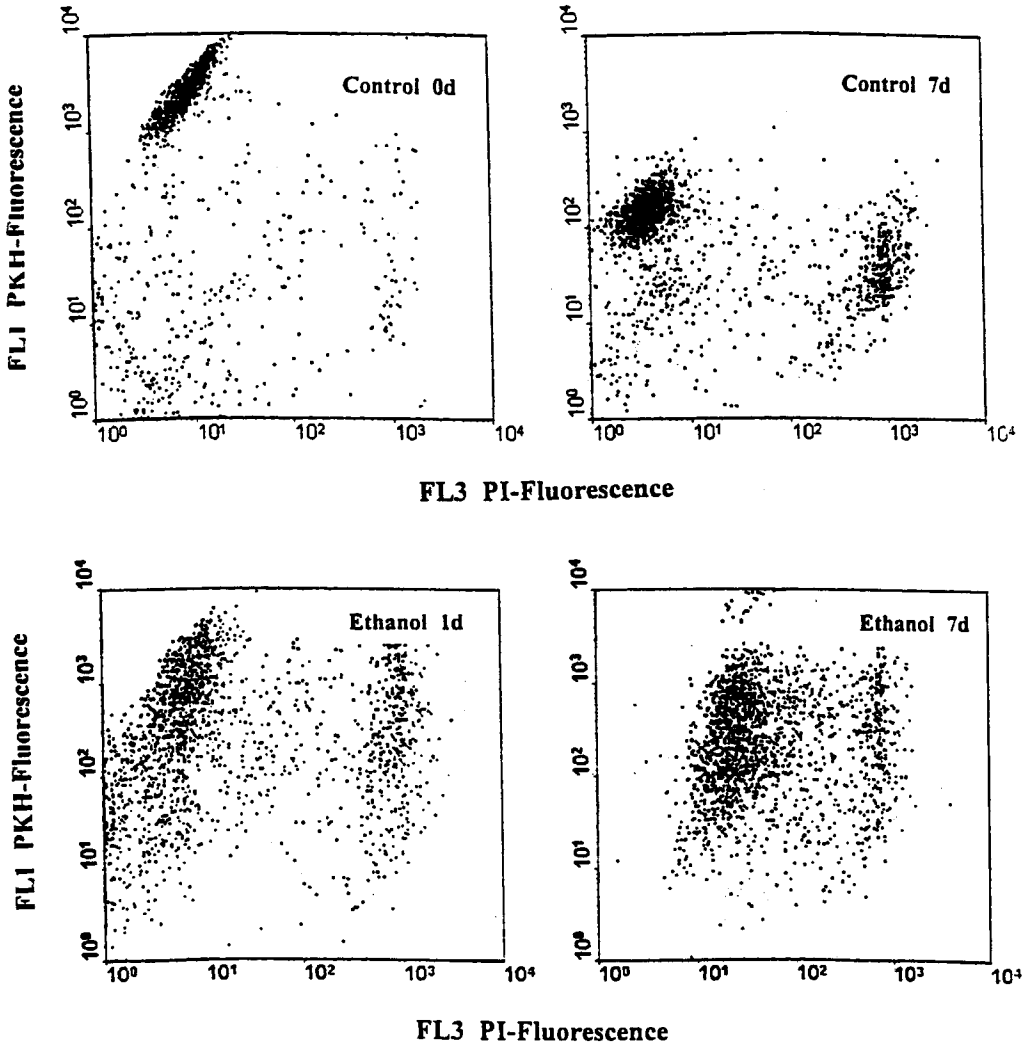

Figure 4. Dot plots of PKH-labelled HL-60 cells. The control cells (top) proliferate and dilute the PKH label, and the PKH fluorescence decreases accordingly. In 3% ethanol-treated cells (bottom) the cells are apoptotic or dead after 7 days as can be seen from the increased PI fluorescence indicating membrane leakage. The PKH fluorescence has assumed a wide distribution but the overall decrease is only minor after 7 days.

membrane or label. After 7 days' ethanol treatment (Figure 4, lower right panel) all cells became leaky to PI, but rather few cells were completely leaky and dead (cluster at high PI fluorescence). The PKH-fluorescence was only slightly lower than after 1 day of treatment, indicating that the cells have maintained their membranes fairly intact. The percentages of live, apoptotic, and apoptotic dead cells were the same as found in the curves for cells without PKH-label indicating that PKH labelling has no effect. Figure 5 shows that the PKH-fluorescence per cell of apoptotic and apoptotic dead cells remained nearly constant from day 1 to day 8, indicating that these cells retained their membrane. The control cells, on

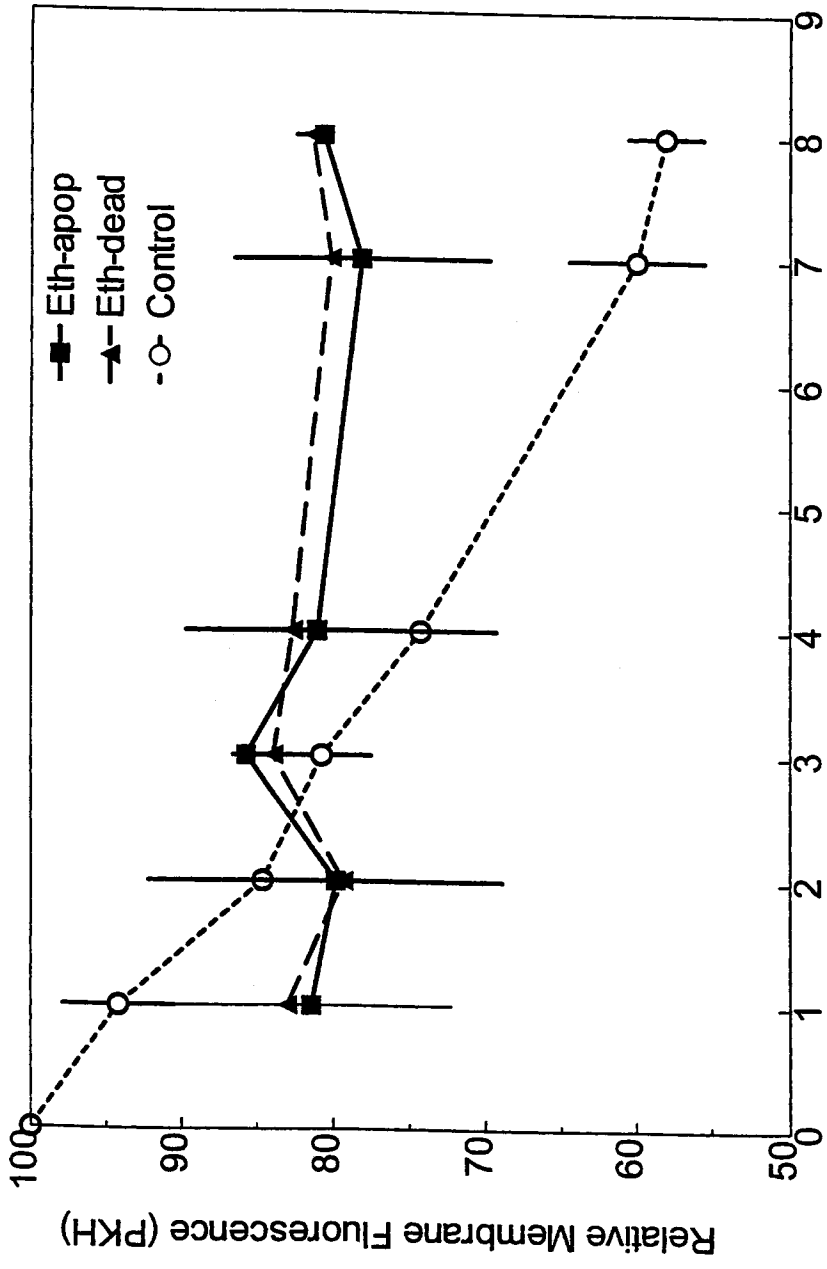

Figure 5. HL-60 cells membrane labelled by PKH and induced to apoptosis by 3% ethanol maintain most of their PKH label up to 8 days, indicating that apoptotic cells decay very slowly and keep their membrane leaky but otherwise intact. Ethanol apopotosis are the cells with intermediate PI staining, Ethanol dead are the cells with maximal PI staining (see Figure 4). Control cells divide and therefore dilute their PKH-label with time. PKH fluorescence was measured in log mode, means and SD from three experiments.

the other hand, proliferated and therefore diluted the PKH label. The straight line reflects the exponential growth as PKH fluorescence was measured in the log mode.

To assess the fate of apoptotic fragments, the same samples were also measured in the FSC-log mode. In the top right panel of Figure 6, the regions of different particle size are shown. R1 represents whole cells, R2, R3, R4 are cell fragments, about 1/10, 1/100, and 1/1000th the size of a complete cell, respectively. For this untreated control, the majority of particles are in R1 (middle left panel shows the related FL3–FL1), and represent highly labelled live cells. The middle right panel was gated from R2, and the bottom left panel from R3; the fragments in both regions do not show correlation between fluorescence 3 (DNA) and fluorescence 1 (PKH). The particles gated from R4 have a low DNA content (if any), however, PKH is widely distributed, indicating larger membrane parts in the fragments with high FL1. The same dot plots and gates of regions according to size of particles for ethanol-treated cells are shown in Figure 7. After 2 days' ethanol treatment, only very few cells are still alive (they appear in the R1 gated dot plot – middle left panel – in the upper left corner). Most of the whole cells from R1 are apoptotic or apoptotic dead with high fluorescence 3. The regions R2 to R4 look quite different from those of the control cells. There is a strong correlation of fluorescence 3 and fluorescence 1 in R4 (bottom right panel) and a less strong correlation in R3 (bottom left panel) and R2 (middle right panel). This proves that the apoptotic fragments contain DNA and PKH-labelled membranes. Cells without PKH-label show much reduced green fluorescence and would not appear in this dot plot (data not shown).

The relative numbers of cells and cell fragments in ethanol-treated cultures are shown in Figure 8; these were calculated from the percentages of fragments as explained in Figure 7 and the total number of cells counted in the Coulter Counter. This latter number was assumed to be equal to the number of cells measured in the region R1; whole cells. From Figure 8a, a slight decrease of whole cells and large fragments can be seen. The number of small fragments, however, increases. This points to a dynamic process with whole cells and large fragments broken up into smaller fragments and the small fragments dissolved. However, the net effect resulted in a slight increase of small fragments.

DISCUSSION

The degradation of DNA and the condensation of chromatin occurred simultaneously after the induction of apoptosis in HL-60 cells. The first apoptotic cells appeared 4 h after induction with ethanol, then the percentage of apoptoses continuously increased up to close to 100% at 48 h (Figure 1). All cell cycle phases were affected in the same way as can be seen from the normal cell histograms of the sub G_1 peak measurement. When CAM was used to induce apoptosis, the S phase cells were the first to become apoptotic, which is well known (Del Bino, Lassota & Darzynkiewicz 1991). However, after about 14 h of treatment the percentage of apoptotic cells increased further. To reveal whether CAM had triggered G_1 cells into apoptosis, chase experiments were carried out. The cells were treated with CAM for 4 h, then the medium was replaced with fresh medium without CAM. As Figure 2 shows the S phase cells are apoptotic after 4 h, however, after an additional 14 h without CAM nearly all of the G_1 and G_2 cells are also apoptotic. This indicates that CAM induces apoptosis in S phase cells almost immediately, and in G_1 and G_2 phases with a 10–20 h delay. A similar finding was reported by Halicka *et al.* (1997), although the authors did not examine the kinetics in detail.

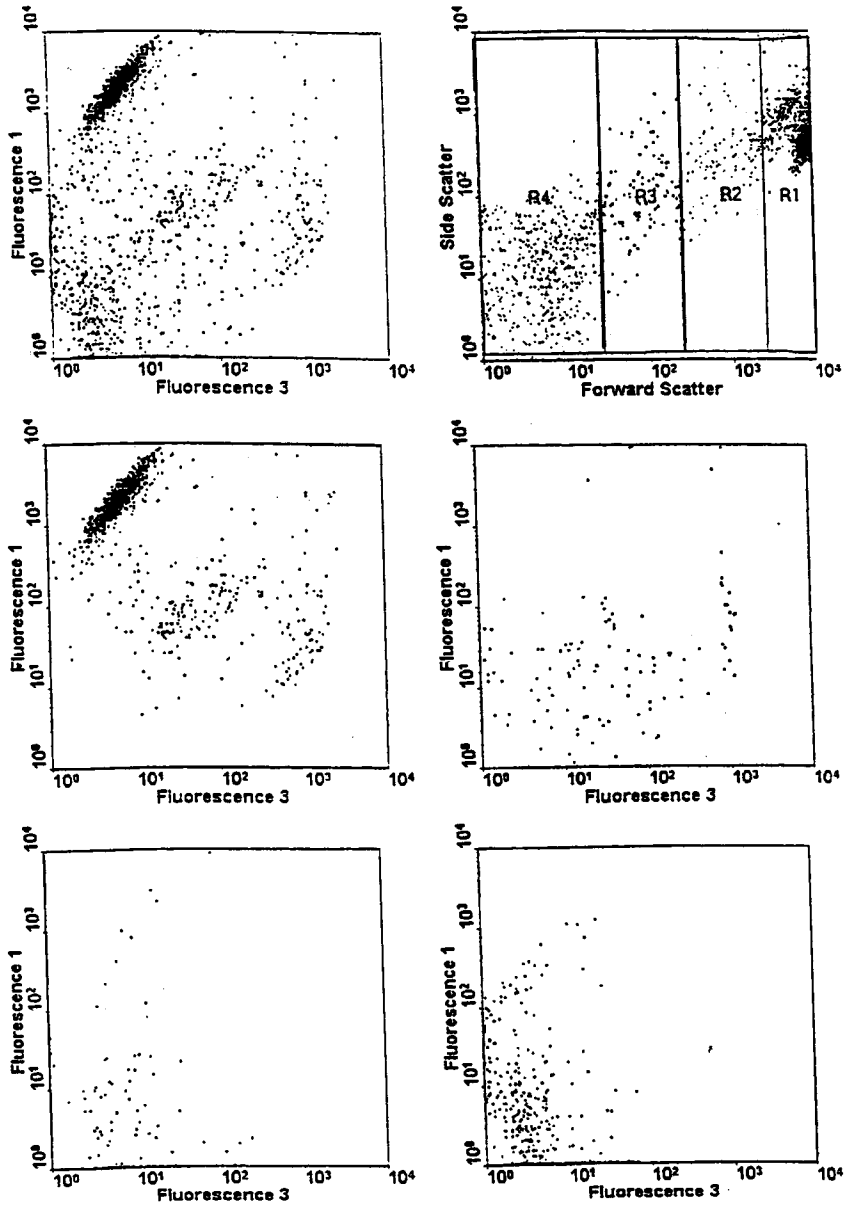

Figure 6. Full size cells, shrunk cells, and small particles – putative apoptotic bodies – in an untreated control 2 days after split, live cells were membrane-labelled with PKH and stained with PI. PKH-labelled HL-60 cell culture was measured by setting FSC to the logarithmic mode. In the FSC–SSC dot plot (upper right) regions R1 to R4 were set, representing whole cells in R1 and particles roughly 1/10, 1/100, and 1/1000th the size of a cell in regions 2, 3, 4, respectively. The middle and bottom panels show the FL3–FL1 dot plots of the regions R1 (middle left), R2 (middle right), R3 (bottom left), and R4 (bottom right). All cells are shown top left. The great majority of live cells with high PKH label (FL1) and exclusion of PI (FL3) appears in R1 in the upper left cluster, a few apoptotic and apoptotic dead cells can be seen in the centre and the right side, respectively. The FL1 of all these particles is considerably higher than control particles without PKH, indicating that they include part of the cell membrane.

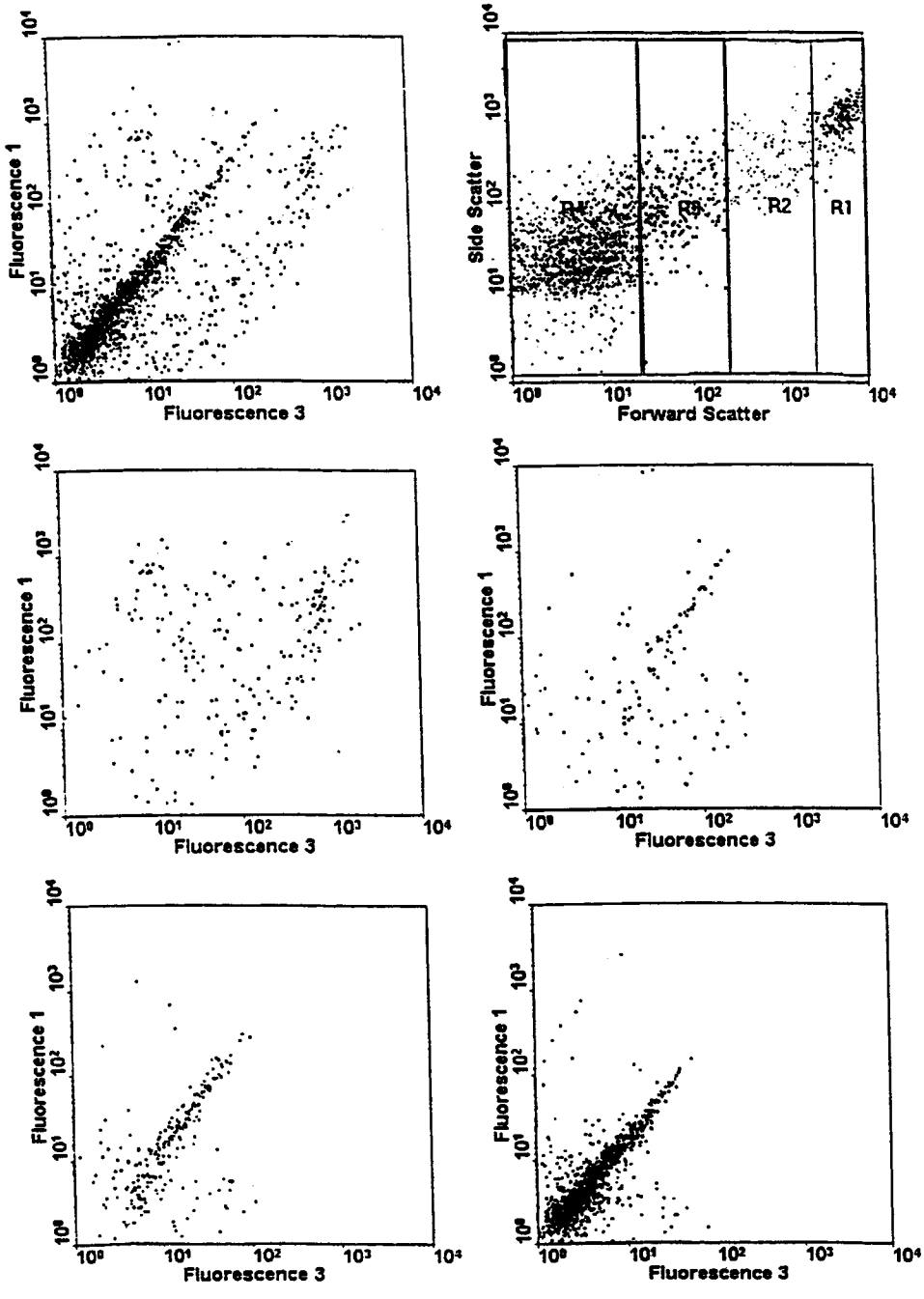

Figure 7. FSC log measurement of HL-60 cells labelled with PKH, then induced to apoptosis by 3% ethanol for 2 days, and stained with PI. The regions in FSC–SSC are the same as in Figure 6. In contrast to untreated cells, FL3 and FL1 are correlated in regions R2–R4 indicating that the apoptotic bodies consist of DNA and membrane.

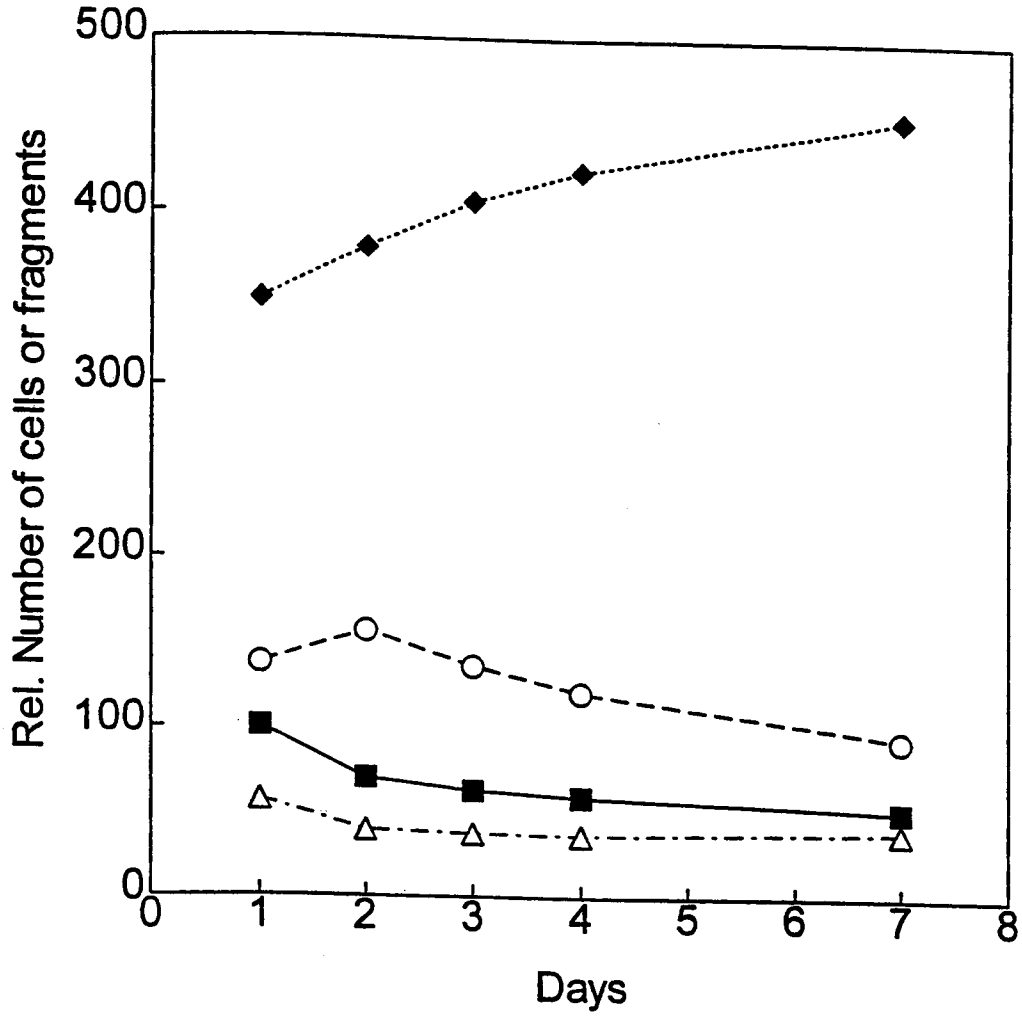

Figure 8. Number of cells (■) and cell fragments (Δ region 2 in Figure 6, FSC-size about 1/10th of whole cells; ○ region 3, FSC-size 1/100th of whole cells; ◆ region 4, FSC-size 1/1000th of whole cells) after induction of apoptosis by 3% ethanol in HL-60 cells. The number of whole cells was counted in a Coulter counter, the percentage of cells and fragments determined by FACScan. The number of whole cells at day 1 was normalized to 100.

The simultaneous occurrence of chromatin condensation as measured by AO staining and DNA degradation as measured by the sub G_1 peak method (and the dUTP labelling) in the present data confirms the results of Hotz *et al.* (1994). Their data even seem to show that chromatin destabilization precedes endonucleolysis, which may be a reflection of histone proteolysis. On the other hand, DNA cleavage is known to increase the sensitivity of DNA to denaturation (Gorczyca *et al.* 1992). The earlier detection of DNA denaturability may, however, also be a result of the better assay sensitivity as compared with the two methods for measuring DNA degradation. It should be noted that DNA denaturability (AO) is not a specific method for apoptotic cells, since DNA in

necrotic cells is also sensitive to denaturation (Hotz *et al.* 1992). In the present experimental approach, no necrotic cells appear, which is confirmed by the identical kinetics of the percentage of apoptotic cells measured by AO, sub G_1 peak, TUNEL, and morphology.

The temporal sequence of mitochondrial membrane potential loss (MPLM), PSE, chromatin condensation, and DNA degradation was studied by Castedo *et al.* (1996). They found no way to dissociate MPLM and PSE. Interference with mitochondrial permeability transition, the mechanism that accounts for MPLM, also prevented PSE, indicating that MPLM directly influenced the downstream process of PSE. The present data are in accordance with this observation. The percentage of cells with PSE increases about 15 h later than that of cells with MPLM. Chromatin condensation and DNA fragmentation depended on MPLM in a similar way according to Castedo *et al.* (1996). This was shown in a cell-free system including purified mitochondria and nuclei, where mitochondria undergoing permeability transition were sufficient to induce chromatin condensation and DNA fragmentation in the nuclei (Zamzami *et al.* 1996). The present results are in contradiction with these observations, and mitochondria MPLM occurred about 4 h later than chromatin condensation and DNA degradation. However, PSE was delayed much more (Figure 1). This is in line with the observations of van Engeland *et al.* (1998) that PSE is a downstream effect of lamin breakdown. At the present time, it seems that various pathways exist that may lead to different time courses (Koopman *et al.* 1994, Vanags *et al.* 1996) and some indicators may appear by a slow build up rather than a sudden change (Frey 1997). Th present data clearly support a slow build up of PSE and mitochondria MPL while chromatin condensation and DNA degradation occur within a short increment of time in all cells induced to apoptosis. The processes through which CAM triggers apoptosis, the temporal sequences of caspase activation, and the relation of caspases to DNA-degradation remain controversial or unknown (Furuya, Ohta & Ito 1997, Sheard 1997). It is also not known how ethanol triggers apoptosis; however, a direct permeability change is excluded by the data – rather, the kinetics are similar to CAM induction.

Decomposition of apoptotic HL-60 cells was much slower than execution of the more early steps during the apoptosis process. An exponential decay with a $T_{½}$ of 17.6 h was measured, indicating that some apoptotic cells remained in the medium for several days. *In vivo*, the lifetime of apoptotic cells is much shorter. They are phagocytosed by macrophages or their neighbouring cells in solid tissues. The mean duration of observable histological stages was about 3 h (Bursch *et al.* 1990). Apoptotic cells in the peripheral blood may have a longer lifetime. However, as exposure of PS on their surface triggers recognition by macrophages (Fadok *et al.* 1992), phagocytosis is probably more a matter of hours than days.

Cell fragments and small apoptotic bodies were found to have a similar lifetime in suspension to whole cells (Figure 8). Only the smallest (1/1000th the size of whole cells according to FSC) increase in number with time. This indicates a continuous but slow decomposition of larger fragments. PKH labelling showed that all the fragments and even the smallest apoptotic bodies contained DNA and membranes (Figures 6 and 8). Taking together all the results of the lifetime studies, it seems that the apoptosis programme has no further steps after the partial DNA degradation and decomposition of cells into apoptotic bodies of various sizes, from nearly whole cells to particles about 1/1000th of a cell. Moreover, DNA degradation itself seems to cease after the initial burst, otherwise there would be no apoptotic bodies containing DNA up to 7 days after induction of apoptosis.

ACKNOWLEDGEMENTS

The authors thank Renate Erb for professional help with the manuscript.

REFERENCES

BOERSMA AWM, NOOTER K, OOSTRUM RG, STOTER G. (1996) Quantification of apoptotic cells With fluorescein isothiocyanate-labeled annexin V in chinese hamster ovary cell cultures treated with cisplatin. *Cytometry* **24,** 123.

BURSCH W, PAFFE S, PUTZ B, BARTHEL G, SCHULTE-HERMANN R. (1990) Determination of the length of the histological stages of apoptosis in normal liver and in altered hepatic foci of rats. *Carcinogenesis* **11,** 847.

CASTEDO M, HIRSCH T, SUSIN SA *et al.* (1996) Sequential acquisition of mitochondrial and plasma membrane alterations during early lymphocyte apoptosis. *J. Immunol.* **157,** 512.

DARZYNKIEWICZ Z. (1990) Acid-induced denaturation of DNA *in situ* as a probe of chromatin structure. *Meth. Cell Biology* **33,** 337.

DARZYNKIEWICZ Z, BRUNO S, DEL BINO G *et al.* (1992) Features of apoptotic cells measured by flow cytometry. *Cytometry* **13,** 795.

DARZYNKIEWICZ Z. (1995) Apoptosis in antitumour strategies: modulation of cell cycle and differentiation. *J. Cell Biochem.* **58,** 151.

DEL BINO G, LASSOTA P, DARZYNKIEWICZ Z. (1991) The S-phase cytotoxicity of camptothecin. *Exp. Cell Research* **193,** 27.

FADOK VA, VOELKER DR, CAMPBELL PA, COHEN JJ, BRATTON DL, HENSON PM. (1992) Exposure of phosphatidylserine on the surface of apoptotic lymphocytes triggers specific recognition and removal by macrophages. *J. Immunol.* **148,** 2207.

FISHER DE. (1994) Apoptosis in cancer therapy: crossing the threshold. *Cell* **78,** 539.

FRANKFURT OS, BYRNESS JJ, SECKINGER D, SUGARBAKER EV. (1993) Apoptosis (programmed cell death) and the evaluation of chemosensitivity in chronic lymphocytic leukemia and lymphoma. *Onc. Res.* **5,** 37.

FREY T. (1997) Correlated flow cytometric analysis of terminal events in apoptosis reveals the absence of some changes in some model systems. *Cytometry* **28,** 253.

FURUYA Y, OHTA S, ITO H. (1997) Apoptosis of androgen-independent mammary and prostate cell lines induced by topoisomerase inhibitors: common pathway of gene regulation. *Anticancer Res.* **17,** 2089.

GORCZYCA W, BRUNO S, DARZYNCIEWICZ RJ, GONG J, DARZYNCIEWICZ Z. (1992) DNA strand breaks occuring during apoptosis: their early *in situ* detection by the terminal deoxynucleotidyl transferase and nick translation assays and prevention by serine protease inhibitors. *Int. J. Oncol.* **1,** 639.

HALICKA HD, SEITER K, FELDMAN EJ *et al.* (1997) Cell cycle specificity of apoptosis during treatment of leukaemias. *Apoptosis* **2,** 25.

HORAN PK, MELNICOFF MJ, JENSEN BD, SLEZAK SE. (1990) Fluorescent cell labeling for *in vivo* and *in vitro* cell tracking. *Method. Cell Biol.* **33,** 469.

HOTZ MA, TRAGANOS F, DARZYNKIEWICZ Z. (1992) Changes in nuclear chromatin related to apoptosis or necrosis induced by the DNA topoisomerase II inhibitor fostriecin in MOLT-4 and HL-60 cells are revealed by altered DNA sensitivity to denaturation. *Exp. Cell Res.* **201,** 184.

HOTZ MA, GONG J, TRAGANOS F, DARZYNKIEWICZ Z. (1994) Flow cytometric detection of apoptosis: comparison of the assays of *in situ* DNA degradation and chromatin changes. *Cytometry* **15,** 237.

KERR JFR, WYLLIE AH, CURRIE AH. (1972) Apoptosis, a basic biological phenomenon with wider implications in tissue kinetics. *Br. J. Cancer* **26,** 239.

KERR JFR, WINTERFORD CM, HARMON V. (1994) Apoptosis, its significance in cancer and cancer therapy. *Cancer* **73,** 2013.

KOOPMAN G, REUTELINGSPERGER CPM, KUIJTEN GAM, KEEHNEN RMJ, PALS ST, VAN OERS MHJ. (1994) Annexin V for flow cytometric detection of phosphatidylserine expression on B cells undergoing apoptosis. *Blood* **84,** 1415.

LI X, GONG J, FELDMAN E, SEITER K, TRAGANOS F, DARZYNKIEWICZ Z. (1994) Apoptotic cell death during treatment of leukemias. *Leuk. Lymph. (Suppl.)* **1,** 65.

MAJNO G, JORIS I. (1995) Apoptosis, oncosis, and necrosis. An overview of cell death. *Am. J. Pathology* **146,** 3.

MIGNOTTE B, VAYSSIERE J-L. (1998) Mitochondria and apoptosis. *Eur. J. Biochem.* **252,** 1.

POOT M, GIBSON LL, SINGER VL. (1997) Detection of apoptosis in live cells by MitoTracker (TM) Red CMXRos and SYTO dye flow cytometry. *Cytometry* **27,** 358.

SHEARD MA. (1997) Apoptosis update: to be, or not to be, and how to arrange the latter. *Neoplasma* **44,** 202.

THOMPSON EB. (1998) The many roles of c-Myc in apoptosis. *Annu. Rev. Physiol.* **60,** 575.

VAN ENGELAND M, NIELAND LJW, RAMAEKERS FCS, SCHUTTE B, REUTELINGSPERGER CPM. (1998) Annexin V-affinity assay: a review on an apoptosis detection system based on phosphatidylserine exposure. *Cytometry* **31,** 1.

VANAGS DM, PORN ARES MI, COPPOLA S, BURGESS DH, ORRENIUS S. (1996) Protease involvement in fodrin cleavage and phosphatidylserine exposure in apoptosis. *J. Biol. Chem.* **271,** 31075.

WYLLIE AH. (1992) Apoptosis and the regulation of cell numbers in normal and neoplastic tissues: an overview. *Cancer Metast. Rev.* **11,** 95.

ZAMAI L, FALCIERI E, MARHEFKA G, VITALE M. (1996) Supravital exposure to propidium iodide identifies apoptotic cells in the absence of nucleosomal DNA fragmentation. *Cytometry* **23,** 303.

ZAMZAMI N, SUSIN SA, MARCHETTI P *et al.* (1996) Mitochondrial control of nuclear apoptosis. *J. Exp. Med.* **183,** 1533.